

Dynamic controls on erosion and deposition on debris-flow fans

Peter Schürch^{1,2*}, Alexander L. Densmore¹, Nicholas J. Rosser¹, and Brian W. McArdell²

¹Department of Geography and Institute of Hazard, Risk, and Resilience, Durham University, South Road, Durham DH1 3LE, UK

²Federal Institute for Forest, Snow and Landscape Research (WSL), Zürcherstrasse 111, 8903 Birmensdorf, Switzerland

ABSTRACT

Debris flows are among the most hazardous and unpredictable of surface processes in mountainous areas. This is partly because debris-flow erosion and deposition are poorly understood, resulting in major uncertainties in flow behavior, channel stability, and sequential effects of multiple flows. Here we apply terrestrial laser scanning and flow hydrograph analysis to quantify erosion and deposition in a series of debris flows at Illgraben, Switzerland. We identify flow depth as an important control on the pattern and magnitude of erosion, whereas deposition is governed more by the geometry of flow margins. The relationship between flow depth and erosion is visible both at the reach scale and at the scale of the entire fan. Maximum flow depth is a function of debris-flow front discharge and pre-flow channel cross-section geometry, and this dual control gives rise to complex interactions with implications for long-term channel stability, the use of fan stratigraphy for reconstruction of past debris-flow regimes, and the predictability of debris-flow hazards.

INTRODUCTION

Debris flows are ubiquitous hazards in mountain areas, not least because of their ability to avulse from an existing channel and inundate adjacent areas on debris-flow fans (Rickenmann and Chen, 2003; Jakob and Hungr, 2005). The avulsion probability is controlled mainly by the ratio of flow peak discharge and channel conveyance capacity. While the latter can be estimated from field measurements (Whipple and Dunne, 1992), both parameters can change rapidly during a flow due to erosion and deposition along the flow path (Fannin and Wise, 2001). This not only makes it difficult to predict the temporal evolution of an individual flow, but also changes the boundary conditions for the next flow in that channel. There results a critical need to understand the dynamic relationships and feedbacks between debris-flow volume and the changes in channel topography due to erosion and deposition as the flows traverse a fan.

Previous studies have focused more on debris-flow deposition than on the mechanics of erosion, and published work on erosion is partly contradictory. Takahashi (2007) found that the concentration of coarse particles in a debris flow increases with bed slope, and that erosion is only possible when the flow is undersaturated in coarse particles. Field observations, however, indicate that erosion occurs mostly during passage of the granular flow front (Berger et al., 2011), and is likely associated with impacts of coarse sediment on the bed. Iverson et al. (2011) explored the role of bed properties and found a positive correlation between erosional scour depth and bed water content. Debris-flow deposition has been related to channel gradient (Cannon, 1989; Fannin and Wise, 2001; Hungr et al., 2005; Hürlimann et al., 2003), down-

stream channel widening (Cannon, 1989; Fannin and Wise, 2001), or flow volume, based on an observed power-law relationship between flow volume and total inundated area (Griswold and Iverson, 2007). More generally, detailed monitoring of experimental flows (Major and Iverson, 1999) and physically based description of fluid-solid mixtures (Iverson, 1997) have related flow mobility to granular temperature, defined as the mean square of particle velocity fluctuations, and excess pore-fluid pressure (McCoy et al., 2010). These effects are counteracted by friction at the dry coarse-grained flow margins (Major and Iverson, 1999).

The objective of this study is to understand the interaction between a debris flow and the

channel bed by systematically measuring erosion and deposition in a series of natural flows at both the reach and fan scales. We hypothesize, based on the results of Berger et al. (2011), that local bed elevation change is related to basal shear stress (and thus to maximum flow depth) and flow volume. We use a terrestrial laser scanner (TLS) to determine high-resolution reach-scale measurements of erosion and deposition in a natural channel caused by four debris flows. We then relate these data both to flow depth and to fan-scale flow volume changes estimated from debris-flow hydrographs.

STUDY AREA

The Illgraben debris-flow fan is in the Rhone valley, Switzerland (Fig. 1), and has a long history of debris flows (Marchand, 1871; Lichtenhahn, 1971). The fan has an area of 6.6 km² with a radius of 2 km and a gradient that decreases from 10% to 8% downfan (Schlunegger et al., 2009). The bedrock geology in the catchment is dominated by schist, dolomite breccia, and quartzite (Gabus et al., 2008). The lowermost bedrock along the Illgraben channel crops out just below a sediment retention dam (check dam, CD1, Fig. 1); downstream the channel bed consists of unconsolidated sediments. Convective storms from May to September trigger three to five debris flows per year (McArdell et al.,

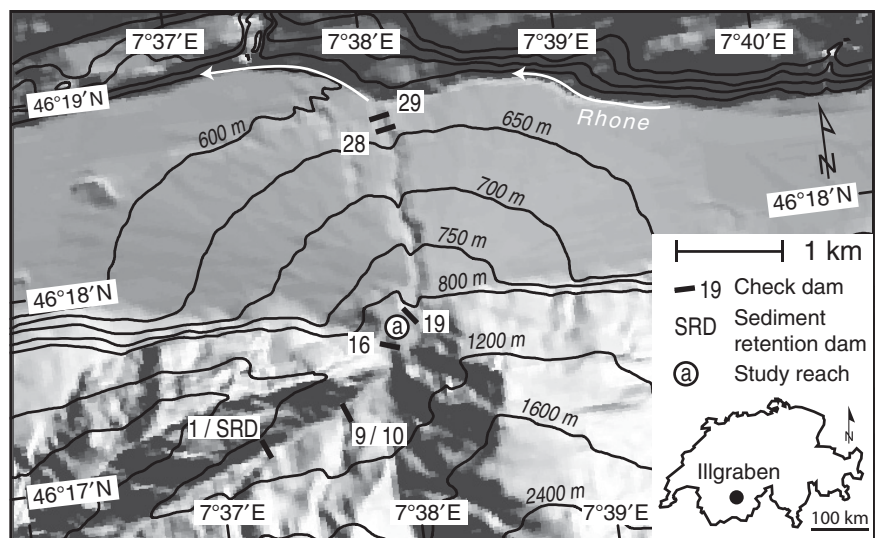


Figure 1. Overview of Illgraben catchment and fan in southeastern Switzerland. Tributary joining downstream of check dam (CD10) is inactive due to hydropower dam in headwaters. Geophones are mounted on CD1, CD9, CD10, CD28, and CD29. Flow stage measurements are taken at CD10 (radar) and CD29 (laser and radar). Study reach is located between CD16 and CD19. Contour interval is 50 m on fan and 400 m for altitudes above 800 m above sea level.

*E-mail: p-s@gmx.ch.

2007). In the 1970s, a series of concrete check dams were constructed to limit erosion and control the channel position on the fan (Lichtenhahn, 1971). Flow hydrograph and onset data are available from two gauging stations at CD10 near the fan apex (Fig. 1; Badoux et al., 2009) and CD29 at the fan toe (McArdell et al., 2007). Since 2007 we have monitored the channel bed using TLS in an unconfined 300 m study reach between CD16 and 19 (Fig. 1).

METHODS

We surveyed the study reach before and after debris flows using a Trimble GS200 TLS, yielding point clouds of $\sim 10^7$ vertices per survey. Data from individual scan positions and subsequent surveys were merged into one coordinate system using an iterative closest point matching algorithm (Besl and McKay, 1992). We gridded the data to a 0.2-m-resolution digital elevation model (DEM) and calculated difference models (Fig. 2) from subsequent surveys; this yields a conservative estimate for erosion because it includes deposition in the falling limb of the flow hydrograph (Berger et al., 2011). For each flow, we mapped maximum inundation limits from levees and mudlines along the channel, and interpolated these to a 0.2-m-resolution maximum flow stage surface. Our estimated uncertainty on this surface is ± 0.25 m, given the difficulties in identifying the mudline in the field due to splashing and poor preservation. The maximum flow stage surface is a lower estimate as the flow surface is generally convex up in cross section. Flow depth was taken as the difference between the maximum flow stage surface and the pre-event DEM. We analyzed the relationship between flow depth and channel change via a cell-by-cell comparison of flow depth with the difference model (Fig. 3A).

To understand how fan-scale flow volume change relates to flow properties, we estimated volumes and debris-flow front heights from the first surge for 14 debris flows in 2007–2009 (Table DR1 in the GSA Data Repository¹) from flow hydrographs measured at the CD10 and CD29 gauging stations. From measurement of the front velocity of each flow, we calibrated a Manning-type friction relation (Schlunegger et al., 2009) to estimate mean flow velocity as a function of flow stage (see the Data Repository). The friction relation is then used to integrate the hydrograph over the event duration to obtain the total flow volumes at both the apex (CD10) and toe (CD29) of the fan.

¹GSA Data Repository item 2011241, Table DR1, data for debris flows discussed in the text, and additional percentile and density plots for individual events, is available online at www.geosociety.org/pubs/ft2011.htm, or on request from editing@geosociety.org or Documents Secretary, GSA, P.O. Box 9140, Boulder, CO 80301, USA.

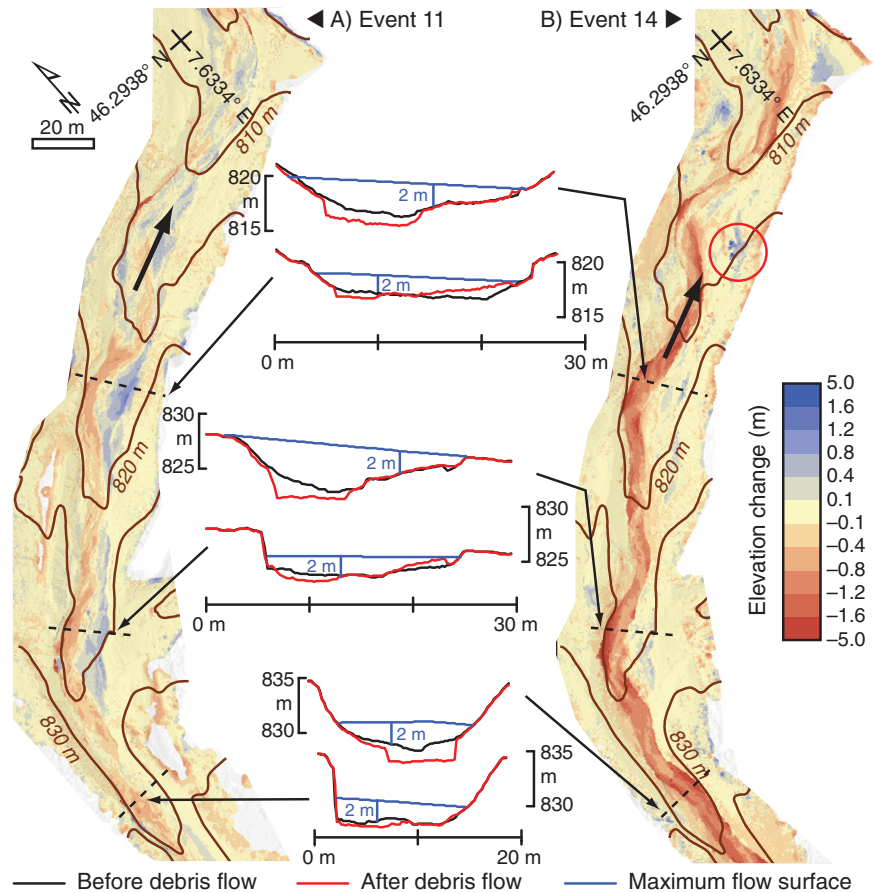


Figure 2. Difference digital elevation models (0.2 m cell size). A: For flow 11. B: For flow 14. For flow details, see Table DR1 (see footnote 1). Background hillshade image represents pre-event topography. Color scale values indicate surface elevation change during flow; elevation change $\leq \pm 0.1$ m is shown in white due to uncertainty caused by small-scale surface roughness. Center panels show elevation change in selected cross sections; black line indicates pre-event topography, red line indicates post-event topography, and blue line indicates maximum flow stage in channel. Contour interval is 5 m. Red circle (panel B) shows overbank boulder deposition.

RESULTS

The difference DEMs for events 11 and 14 (Fig. 2) show that both events caused net erosion within the study reach, leading to increases in flow volume of $87 \pm 6 \text{ m}^3$ and $2039 \pm 4 \text{ m}^3$, respectively, but that the spatial patterns of erosion and deposition are very different. Event 11 shows alternating regions of erosion and deposition, with erosion along the deepest parts of the channel and on the outside of bends, and discontinuous levee deposits along the flow margins and on shallow terraces (Fig. 2A). The maximum discharge in this event was $\sim 60 \text{ m}^3 \text{ s}^{-1}$ calculated at CD10. In event 14, the deepest parts of the channel were eroded continuously throughout the reach; zones of deposition correspond to localized overbank spill and several large boulders (diameter > 2 m) were emplaced along the flow margins (Fig. 2B). The average flow depth in the channel was substantially larger than in event 11, and we estimate a maximum discharge of $\sim 630 \text{ m}^3 \text{ s}^{-1}$ at CD10.

By combining estimated maximum flow depth in each grid cell with the measured elevation change in that cell for events 9, 11, 12, and 14, we can evaluate the effect of flow depth on the probability of erosion or deposition (Fig. 3A). The data illustrate two important observations—that substantial erosion is more likely with increased flow depth, but also that a broad range of outcomes is possible at any given flow depth.

Flow depth also appears to control debris-flow behavior at the fan scale. Of the 14 events in Figure 3B, 11 led to net deposition on the fan and 3 (5, 9, 13) to net erosion when comparing flow volumes at CD10 and CD29. All erosive events had front heights > 2.3 m, and all depositional events (except 14) had front heights < 2.7 m. Event 14 consisted of two surges within the first 17 s with front heights of 2.3 m and 5.2 m. By CD29, only a single surge was discernible, with a front height of 2.5 m. At the fan scale this event was clearly depositional

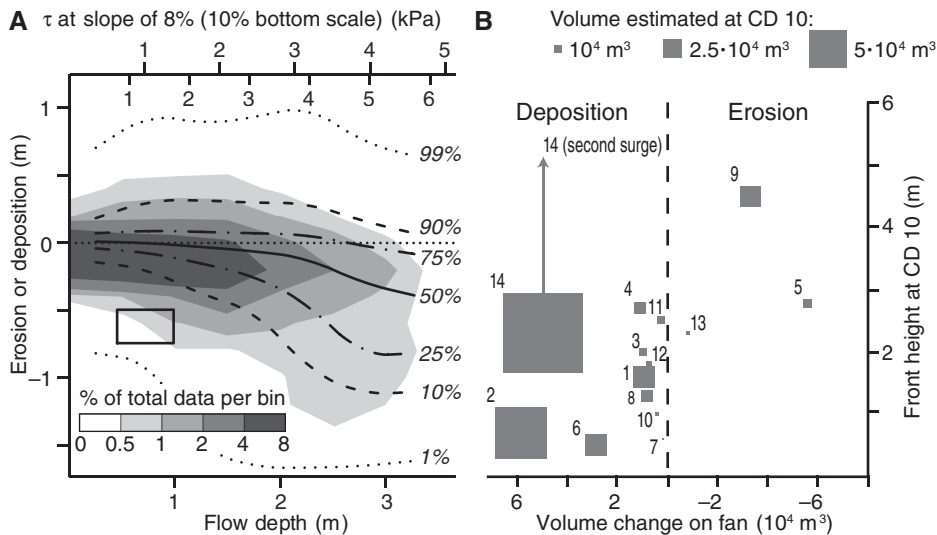


Figure 3. A: Percentile plot of cell-by-cell comparison of elevation change (erosion or deposition) against maximum flow depth for events 9, 11, 12, and 14. Top axis shows estimated basal shear stress for channel slopes of 8% (above) and 10% (below). Gray shades show contours of raw data density based on bin size of 0.5 m in flow depth (shown by solid box). Ensemble of percentile lines illustrates frequency distribution of elevation change at any given flow depth. Total number of data points is 565,344. For individual events, see Fig. DR3 (see footnote 1). B: Fan-scale flow volume change against flow front depth at check dam 10 (CD10) for 14 events between 2007 and 2009. Numbers next to symbols indicate event number. For flow details, see Table DR1. Box width indicates event volume at CD10. Volumes include both water and sediment. Arrow indicates height of second surge in event 14.

(Fig. 3B). However, visual inspection of the channel showed that it was highly erosive on the upper part of the fan (between CD10 and 19), including the study reach (Fig. 2B), while downstream of CD19 we observed widespread deposition on inset terraces.

DISCUSSION AND CONCLUSIONS

We have established a unique record showing correlation between flow depth and erosion or deposition in debris flows (Fig. 3A). At flow depths of <1.5 m, the probability distribution function (PDF) of bed elevation change approaches symmetry at ~ 0 : erosion and deposition are equally likely. As flow depth increases, the PDF widens to include the possibility of high erosion values, while the probability of deposition decreases moderately. At a flow depth of 1–2 m, the probability of deposition is as high as 50%, while at a depth of 3 m the probability of deposition is <25%. Flow depth exerts a much stronger influence in the erosional domain: the 10%, 25%, and 50% quantiles of erosion all show an increase at flow depths >2 m. Furthermore, between 2 and 3 m flow depth, the likely amount of erosion at any given probability level approximately doubles.

Flow depth is largest at the debris-flow front (Iverson, 1997; McArdell et al., 2007) and the majority of erosion takes place during its passage (Berger et al., 2011). The flow depth at the front influences the forces acting on the channel bed via three mechanisms: higher basal shear

stress, the impact stresses of coarse particles recirculating in the flow front (Suwa, 1988; Stock and Dietrich, 2006; Hsu et al., 2008), and hydraulic pressure at the flow front that may cause rapid undrained loading (Hung et al., 2005) and liquefaction of the channel bed (Sassa and Wang, 2005). Although all three processes may be relevant here, we lack data on the second and third mechanisms. We can evaluate the first by converting flow depth to basal shear stress (Fig. 3A), defined as $\tau = \rho g h S$, where ρ is density, g is gravity, h is flow depth, and S is channel slope. Taking an observed median density of debris-flow fronts at Illgraben of 1800 kg/m^3 (35 events) and slopes of 8%–10%, we find that substantial erosion takes place when a basal shear stress of 3–4 kPa is exceeded, which is consistent with erosion monitoring near CD29 (Berger et al., 2011). Whether this shear stress reflects an effective strength of bed material, or is instead analogous to a threshold shear stress for fluvial entrainment, is not clear from our data. Other effects such as grain impact (Berger et al., 2011) or antecedent moisture conditions of the bed (Iverson et al., 2011) are also relevant.

In contrast, debris-flow deposition occurs dominantly along the flow margins and where the flows spread over low-relief areas adjacent to the channel (Fig. 2). It has been argued elsewhere (e.g., Cannon, 1989; Major and Iverson, 1999; Fannin and Wise, 2001) that this pattern is consistent with the triggering of deposition by increased friction along the flow margins, and

by changes in local channel geometry. This is illustrated in Figure 2 by substantial deposition in the lower, wider cross sections rather than the narrow upstream section of the reach.

If debris-flow front height is a key variable in determining flow behavior, then what are its primary controls? Front height is proportional to discharge but is dynamically adjusted as the channel cross-section geometry changes along the flow path. Sudden changes in channel geometry can reduce the maximum flow depth and cause both overbank deposition and, critically, a decrease in basal shear stress within the channel, potentially leading to the onset of in-channel deposition (Cannon, 1989). Front height is also likely to vary with the proportion of the coarse sediment fraction. Coarse debris-flow fronts have very low fluid pressures (Iverson, 1997; McArdell et al., 2007), leading to the analogy of these steep and dry flow fronts as mobile dams (Major and Iverson, 1999). As a thought experiment, consider such a mobile dam with a triangular cross section in a channel ~ 4 m deep and 10 m wide, implying a total of $\sim 160 \text{ m}^3$ of material to build. Because coarse particles are recirculated in the flow front (Suwa, 1988; Iverson, 1997), a debris flow probably requires a multiple of this volume to sustain the mobile dam, but even this is a small amount of material compared to typical Illgraben flow volumes (Table DR1). Thus, the loss of even moderate volumes of coarse debris to levee deposition may lead to a fundamental downstream change in behavior as flow height decreases. Event 14, which showed a rapid downstream transition from dominantly erosional to dominantly depositional behavior, may represent an example of this process.

Our findings also have implications for the channel evolution over the course of sequential events. Figure 4 shows per-event and cumulative fan-scale changes in flow volume, indicating three phases of aggradation each followed by an erosive event. The state of the channel

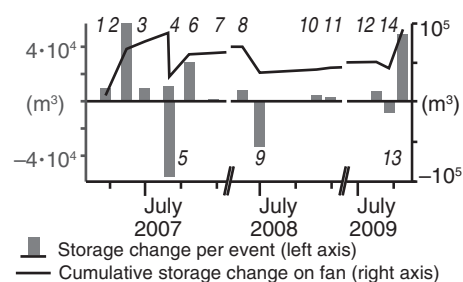


Figure 4. Time series of erosional (negative) or depositional (positive) volume change per event, calculated as difference between volumes at check dam (CD) 10 and CD29 (gray bars) with event numbers (Table DR1; see footnote 1) and cumulative volume change (black line).

changes as a result of these events: in events with a very high front we expect deposition on the channel banks and erosion along the center line (e.g., Fig. 2B); a medium front height in the same channel might only erode along the center line; and events with even smaller flow fronts might gradually fill the channel by deposition of lobes and inset levees. As a result, similar consecutive events entering the apex of the fan will experience a different channel cross section than their predecessors and will undergo different downfan changes in volume increase or loss. The cycles of filling and evacuating the channel observed here are evocative of larger-scale autocyclic storage and release of sediment on alluvial fans (Kim et al., 2006; Kim and Muto, 2007), and have major implications for the preservation of debris-flow fan stratigraphy, even in the absence of temporal variations in external controls such as climate, tectonics, or changes in sediment supply. In addition, the lack of correlation ($R^2 = 0.0004$) between flow volume and front height (Fig. 3B) means that (perhaps counterintuitively) flows with larger total volumes may not necessarily pose the greatest hazard of avulsion. The dependence of flow volume change on the local channel characteristics and the history of previous flows is likely to complicate efforts to define hazard by establishing magnitude-frequency distributions for particular catchments (Zimmermann et al., 1997; Hungr et al., 2008; Jakob and Friele, 2010; Stoffel, 2010) without a better understanding of downstream flow evolution.

ACKNOWLEDGMENTS

Funding for this research has come from Natural Environment Research Council grant NE/G009104/1, Durham University, and a Royal Geographical Society field work grant. The base for Figure 1 is taken from DHM25© 2011 swisstopo (Swiss Federal Office of Topography). We thank T.C. Hales, J. Kean, and an anonymous reviewer for insightful comments.

REFERENCES CITED

- Badoux, A., Graf, C., Rhyner, J., Kuntner, R., and McArdell, B.W., 2009, A debris-flow alarm system for the Alpine Illgraben catchment: Design and performance: *Natural Hazards*, v. 49, p. 517–539, doi:10.1007/s11069-008-9303-x.
- Berger, C., McArdell, B.W., and Schlunegger, F., 2011, Direct measurement of channel erosion by debris flows, Illgraben, Switzerland: *Journal of Geophysical Research*, v. 116, no. F1, F01002, doi:10.1029/2010JF001722.
- Besl, P., and McKay, N., 1992, A method for registration of 3-D shapes: *IEEE Transactions on Pattern Analysis and Machine Intelligence*, v. 14, p. 239–256, doi:10.1109/34.121791.
- Cannon, S.H., 1989, An evaluation of the travel-distance potential of debris flows: *Utah Geological and Mineral Survey Miscellaneous Publication* 89-2, 35 p.
- Fannin, R.J., and Wise, M.P., 2001, An empirical-statistical model for debris flow travel distance: *Canadian Geotechnical Journal*, v. 38, no. 5, p. 982–994, doi:10.1139/cgj-38-5-982.
- Gabus, J., Weidmann, M., Sartori, M., and Burri, M., 2008, Feuille 1287 Sierre–Atlas géologique Suisse; Carte et Notice explicative 111: Wabern, Switzerland, Office Fédéral de Topographie, scale 1:25 000.
- Griswold, J., and Iverson, R., 2007, Mobility statistics and automated hazard mapping for debris flows and rock avalanches: *U.S. Geological Survey Scientific Investigations Report* 2007–5276, 50 p.
- Hsu, L., Dietrich, W.E., and Sklar, L.S., 2008, Experimental study of bedrock erosion by granular flows: *Journal of Geophysical Research*, v. 113, F02001, 21 p., doi:10.1029/2007JF000778.
- Hungr, O., McDougall, S., and Bovis, M., 2005, Entrainment of material by debris flows, in Jakob, M., and Hungr, O., eds., *Debris-flow hazards and related phenomena*: Berlin, New York, Springer, p. 135–158, doi:10.1007/b138657.
- Hungr, O., McDougall, S., Wise, M., and Cullen, M., 2008, Magnitude-frequency relationships of debris flows and debris avalanches in relation to slope relief: *Geomorphology*, v. 96, p. 355–365, doi:10.1016/j.geomorph.2007.03.020.
- Hürlimann, M., Rickenmann, D., and Graf, C., 2003, Field and monitoring data of debris-flow events in the Swiss Alps: *Canadian Geotechnical Journal*, v. 40, p. 161–175, doi:10.1139/t02-087.
- Iverson, R.H., 1997, The physics of debris flows: *Reviews of Geophysics*, v. 35, p. 245–296, doi:10.1029/97RG00426.
- Iverson, R.M., Reid, M.E., Logan, M., LaHusen, R.G., Godt, J.W., and Griswold, J.P., 2011, Positive feedback and momentum growth during debris-flow entrainment of wet bed sediment: *Nature Geoscience*, v. 4, no. 2, p. 116–121, doi:10.1038/ngeo1040.
- Jakob, M., and Friele, P., 2010, Frequency and magnitude of debris flows on Cheekye River, British Columbia: *Geomorphology*, v. 114, p. 382–395, doi:10.1016/j.geomorph.2009.08.013.
- Jakob, M., and Hungr, O., 2005, *Debris-flow hazards and related phenomena*: Springer, Berlin, New York, 170 p.
- Kim, W., and Muto, T., 2007, Autogenic response of alluvial-bedrock transition to base level variation: Experiment and theory: *Journal of Geophysical Research*, v. 112, F03S14, doi:10.1029/2006JF000561.
- Kim, W., Paola, C., Swenson, J.B., and Voller, V.R., 2006, Shoreline response to autogenic processes of sediment storage and release in the fluvial system: *Journal of Geophysical Research*, v. 111, F04013, doi:10.1029/2006JF000470.
- Lichtenhahn, C., 1971, Zwei Betonmauern: die Geschieberückhaltesperre am Illgraben (Wallis), in *Internationales Symposium Interpraevent*: Villach, Austria, F.f.v. Hochwasserbekämpfung, p. 451–456.
- Major, J.J., and Iverson, R.M., 1999, Debris-flow deposition: Effects of pore-fluid pressure and friction concentrated at flow margins: *Geological Society of America Bulletin*, v. 111, p. 1424–1434, doi:10.1130/0016-7606(1999)111<1424:DFDEOP>2.3.CO;2.
- Marchand, A., 1871, Les Torrents des alpes, in *Revue des eaux et forêts, annales forestières*, Paris, no. 10, p. 77–95.
- McArdell, B.W., Bartelt, P., and Kowalski, J., 2007, Field observations of basal forces and fluid pore pressure in a debris flow: *Geophysical Research Letters*, v. 34, L07406, doi:10.1029/2006GL029183.
- McCoy, S.W., Kean, J.W., Coe, J.A., Staley, D.M., Wasklewicz, T.A., and Tucker, G.E., 2010, Evolution of a natural debris flow: In situ measurements of flow dynamics, video imagery, and terrestrial laser scanning: *Geology*, v. 38, p. 735–738, doi:10.1130/G30928.1.
- Rickenmann, D., and Chen, C.L., 2003, Debris-flow hazards mitigation: Mechanics, prediction, and assessment: *Proceedings of the Third International Conference on Debris-Flow Hazards Mitigation*: Davos, Switzerland, September 10–12, 2003: Rotterdam, Millpress, 1392 p.
- Sassa, K., and Wang, G., 2005, Mechanism of landslide-triggered debris flows: Liquefaction phenomena due to the undrained loading of torrent deposits, in Jakob, M., and Hungr, O., eds., *Debris-flow hazards and related phenomena*: Berlin, New York, Springer, p. 81–103, doi:10.1007/3-540-27129-5_5.
- Schlunegger, F., Badoux, A., McArdell, B.W., Gwerder, C., Schnydrig, D., Rieke-Zapp, D., and Molnar, P., 2009, Limits of sediment transfer in an alpine debris-flow catchment, Illgraben, Switzerland: *Quaternary Science Reviews*, v. 28, p. 1097–1105, doi:10.1016/j.quascirev.2008.10.025.
- Stock, J.D., and Dietrich, W.E., 2006, Erosion of steepland valleys by debris flows: *Geological Society of America Bulletin*, v. 118, p. 1125–1148, doi:10.1130/B25902.1.
- Stoffel, M., 2010, Magnitude-frequency relationships of debris flows—A case study based on field surveys and tree-ring records: *Geomorphology*, v. 116, p. 67–76, doi:10.1016/j.geomorph.2009.10.009.
- Suwa, H., 1988, Focusing mechanism of large boulders to a debris-flow front: *Japanese Geomorphological Union Transactions*, v. 9, no. 3, p. 151–178.
- Takahashi, T., 2007, *Debris flow: Mechanics, prediction and countermeasures*: London, New York, Taylor & Francis, 448 p.
- Whipple, K.X., and Dunne, T., 1992, The influence of debris-flow rheology on fan morphology, Owens Valley, California: *Geological Society of America Bulletin*, v. 104, p. 887–900, doi:10.1130/0016-7606(1992)104<0887:TIODFR>2.3.CO;2.
- Zimmermann, M., Mani, P., and Romang, H., 1997, Magnitude-frequency aspects of alpine debris flows: *Eclogae Geologicae Helvetiae*, v. 90, p. 415–420.

Manuscript received 24 January 2011
 Revised manuscript received 30 March 2011
 Manuscript accepted 7 April 2011

Printed in USA